

Thiacrown Pt^{II} complexes with group 15 donor ligands: pentacoordination in Pt(II) complexes†

Gregory J. Grant,*^a Desirée A. Benefield^a and Donald G. VanDerveer^b

Received 20th May 2009, Accepted 13th July 2009

First published as an Advance Article on the web 19th August 2009

DOI: 10.1039/b909875e

We report the synthesis and full characterization for a series of thiacrown complexes of Pt(II) incorporating the fluxional trithiacrown ligand 1,4,7-trithiacyclononane ([9]aneS₃) and several group 15 donor ligands. Reaction of [Pt([9]aneS₃)Cl₂] with a full stoichiometric equivalent of the group 15 donor (L = 2 × AsPh₃, SbPh₃ or 1,2-bis(diphenylarsenio) ethane (dpae) followed by metathesis with NH₄PF₆ yields [Pt([9]aneS₃)L](PF₆)₂. We also report the analogous Pd(II) complex with dpae. Similar reactions of the starting Pt complex with one equivalent of XPh₃ (X = As or Sb) result in complexes of the formula [Pt([9]aneS₃)(XPh₃)(Cl)](PF₆). All six new complexes have been fully characterized by multinuclear NMR, IR, and UV-Vis spectroscopies in addition to elemental analysis and single crystal structural determinations. The X-ray structures of each complex indicate an axial M–S interaction formed by the endodentate conformation of the [9]aneS₃ ligand. The axial M–S distance is highly dependent upon the ancillary donor set. The axial M–S distance shortens with the identity of the group 15 donor ligand according to the trend, Sb < As < P, due to their increasingly poorer donor qualities. The two bis pnictogen complexes, [Pt([9]aneS₃)(AsPh₃)₂](PF₆)₂ and [Pt([9]aneS₃)(SbPh₃)₂](PF₆)₂ form unusual five-coordinate distorted trigonal bipyramids in contrast to the pseudo-five coordinate, elongated square pyramidal structures typically observed in Pt(II) complexes of [9]aneS₃. The distortion arises from intramolecular π–π interactions between the phenyl rings on the two different triphenyl ligands. Chemical shifts in the ¹⁹⁵Pt NMR also show similar periodic relationships which trend progressively upfield as the donor atom becomes larger. As expected, the coordinated [9]aneS₃ ligand shows fluxional behavior in its NMR spectra, resulting in a single ¹³C NMR resonance, despite the asymmetric coordination environment found in both chloro complexes. The line width for the carbon NMR resonance as well as for the ¹⁹⁵Pt NMR peak is highly sensitive to the nature of the group 15 donor, with poorer donors such as SbPh₃ showing significant line broadening. Measurements from the electronic spectra support that the ligand field strength of the pnictogen donor decreases with its increasing size.

Introduction

The coordination chemistry of arsine and stibine ligands provides interesting contrasts with the more commonly studied phosphine ligands. Transition metal complexes of As and Sb ligands has been the subject of several reviews^{1–5} including two recent reviews by Levason and Reid.^{1,2} Complexation behavior of the group 15 donor becomes increasingly less well understood as the pnictogen family is descended due to a more limited set of coordination complexes. With the increasing size of the pnictogen, the ligand shows progressively poorer complexation behavior.^{1,2} Accordingly, the heavier congeners are both poorer σ donors and weaker π acceptors due to the increasing energy gap between their s and p atomic orbitals. The increasing p component weakens the

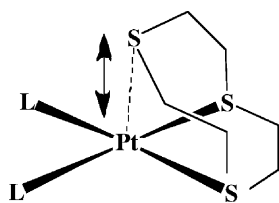
E–C bond (E = group 15 donor) and is further seen with a decrease in the C–E–C bond angles. In addition to these electronic effects, steric effects in group 15 ligands can be important and are typically described in terms of the Tolman cone angle, and the Tolman cone angles for SbPh₃, AsPh₃ and PPh₃ are 138°, 142° and 145°, respectively.^{6,7}

Over the past twenty years, our group and others have prepared an extensive series of Pt(II) and Pd(II) complexes involving the thiacrown ligand, 1,4,7-trithiacyclononane ([9]aneS₃) with a wide range of ancillary ligands including diimines,^{8–11} halides,^{12–16} cyclometalating ligands,^{17,18} and of particular relevance for this report, phosphines such as PPh₃ and a variety of chelating diphosphines.^{19–24} Our goal is to prepare Pt(II) [9]aneS₃ complexes with the heavier group 15 analogues, AsPh₃ and SbPh₃, and contrast their coordination behavior along with their spectroscopic and structural properties, to the previously studied phosphine complexes. In addition, the Pt(II) and Pd(II) [9]aneS₃ complexes with the related bidentate chelator, dpae, 1,2-bis(diphenylarsenio)ethane, the arsenic analog of the popular diphosphine ligand, dppe, are described. This report complements a recent paper from our group describing two Pd(II) triphenylarsine complexes with the trithiacrown.²⁵

^aDepartment of Chemistry, The University of Tennessee at Chattanooga, Chattanooga, TN, 37403, USA. E-mail: Greg-Grant@utc.edu; Fax: 423-425-5234; Tel: 423-425-4143

^bDepartment of Chemistry, Clemson University, Clemson, SC, 29634, USA
† Electronic supplementary information (ESI) available: NMR spectra and structural diagrams. CCDC reference numbers 730838–730842 and 733186. For ESI and crystallographic data in CIF or other electronic format see DOI: 10.1039/b909875e

One interesting feature invariably seen in Pt(II) and Pd(II) thiocrown complexes is the presence of long distance axial sulfur–metal interactions. These interactions arise from an orbital “mismatch” (a term coined by Martin Schröder) between the d^8 transition metal and the facially coordinating trithiacrown.¹² Two of the three sulfur donors form typical equatorial bonds with Pt–S bond distances in the range of 2.2–2.4 Å.[‡] However, the third sulfur donor interacts with Pt(II) at a greater distance which can vary widely, anywhere between 2.6 to 3.4 Å. This distance is highly dependent upon the donor/acceptor properties of the ancillary ligand, and thereby serves as a sensitive structural probe to the electronic nature of the ligand as shown in Scheme 1. Also, the presence of these axial interactions significantly alters the spectroscopic and electrochemical properties of the complex with the stabilization of trivalent oxidation states for Pt and Pd and the presence of unusual d–d electronic transitions in the visible region.^{12,26,27} Furthermore, these types of complexes have been used as models in outer-sphere



Scheme 1 Changes of axial Pt–S distances for the [9]aneS₃ by ancillary ligands.

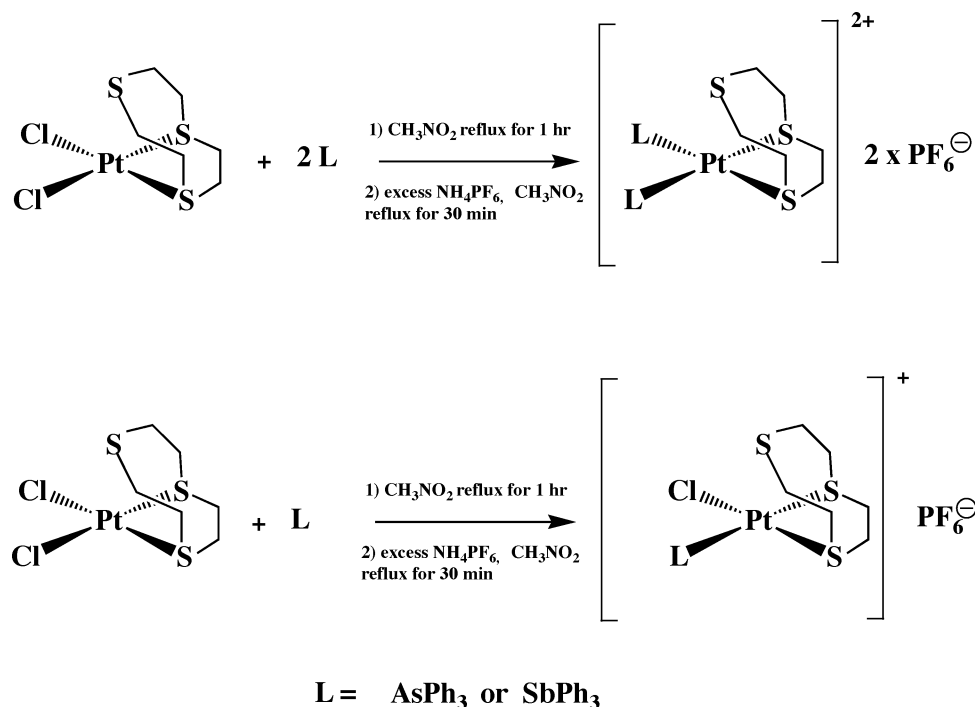
[‡] To our knowledge, there have been 47 Pt(II) [9]aneS₃ complexes structurally characterized including the five new ones reported here. The Pt–S_{ax} distances in these structures range from 2.58 Å to 3.26 Å. Similarly, there have been 24 Pd(II) [9]aneS₃ complexes structurally examined with Pd–S_{ax} distances ranging from 2.67 Å to 3.14 Å.

two-electron oxidations^{10,18,28} and also for associative mechanisms in ligand substitution reactions in d^8 systems.⁸ In a series of [9]aneS₃ metal complexes with group 15 donor ligands, we will focus on how the Pt–S axial distance changes with the electron donating abilities of pnictogen donors and explore periodic relationships. The six new group 15 donor thiocrown complexes described in this report are: [Pt([9]aneS₃)(AsPh₃)₂](PF₆)₂ (**1**), [Pt([9]aneS₃)(AsPh₃)(Cl)](PF₆) (**2**), [Pt([9]aneS₃)(SbPh₃)₂](PF₆)₂ (**3**), [Pt([9]aneS₃)(SbPh₃)(Cl)](PF₆) (**4**), [Pt([9]aneS₃)(dpae)](PF₆)₂ (**5**), and [Pd([9]aneS₃)(dpae)](PF₆)₂ (**6**).

Results and discussion

Syntheses

The synthetic procedures used to prepare the complexes in this study are illustrated in Scheme 2. Ligand substitution by one stoichiometric equivalent of a monodentate group 15 donor (L = AsPh₃ or SbPh₃) results in the displacement of a single chloro ligand from the parent complex [Pt([9]aneS₃)Cl₂] at reflux in nitromethane and readily forms the desired [Pt([9]aneS₃)(L)(Cl)]⁺ complexes in good yields. Similar reactions of the parent complex with either two equivalents of L (or one equivalent of the bidentate dpae ligand) yield complexes with the formula [Pt([9]aneS₃)(L₂)]²⁺. All prepared complexes are subsequently metathesized to the hexafluorophosphate salt which produces better crystalline products. The identities for all six complexes have been confirmed by elemental analyses, a variety of spectroscopic methods, and single-crystal X-ray structures. We would highlight that we are not able to form any isolable Pd(II) complexes with SbPh₃, probably due to the difference in kinetic stability between the Pt and Pd centers. Our group has previously reported the two Pd(II) ([9]aneS₃) complexes [Pd([9]aneS₃)(AsPh₃)₂](PF₆)₂ and [Pd([9]aneS₃)(AsPh₃)(Cl)](PF₆)



Scheme 2 Synthesis of Pt [9]aneS₃ complexes with monodentate group 15 donor ligands.

Table 1 Crystal data, data collection, and refinement parameters for [Pt([9]aneS₃)(AsPh₃)₂](PF₆)₂·2CH₃NO₂ (**1**), [Pt([9]aneS₃)(AsPh₃)(Cl)](PF₆)·1.5CH₃NO₂ (**2**), [Pt([9]aneS₃)(SbPh₃)₂](PF₆)₂·2CH₃NO₂ (**3**), [Pt([9]aneS₃)(SbPh₃)(Cl)](PF₆) (**4**), [Pt([9]aneS₃)(dpae)](PF₆)₂·CH₃CN (**5**), and [Pd([9]aneS₃)(dpae)](PF₆)₂·(CH₃)₂CO (**6**)

Compound	1	2	3	4	5	6
Formula	C ₄₄ H ₄₈ As ₂ F ₁₂ N ₂ ·O ₄ P ₂ PtS ₃	C _{25.5} H _{31.5} AsClF ₆ ·N _{1.5} O ₃ PPtS ₃	C ₄₄ H ₄₈ F ₁₂ N ₂ O ₄ P ₂ ·PtS ₃ Sb ₂	C ₂₄ H ₂₇ ClF ₆ PPtS ₃ Sb	C ₃₄ H ₃₉ As ₂ F ₁₂ NP ₂ PtS ₃	C ₃₅ H ₄₂ As ₂ F ₁₂ OP ₂ PdS ₃
Habit, color	Rod, orange	Chip, orange	Chip, red	Plate, red	Chip, red	Chip, red
Lattice type	Monoclinic	Monoclinic	Triclinic	Orthorhombic	Monoclinic	Triclinic
Space group	<i>P</i> 2 ₁ / <i>c</i>	<i>P</i> 2 ₁ / <i>c</i>	<i>P</i> $\bar{1}$	<i>P</i> 2 ₁ 2 ₁	<i>P</i> 2 ₁ / <i>n</i>	<i>P</i> $\bar{1}$
<i>a</i> /Å	10.6043(13)	8.0987(16)	12.893(3)	8.4062(17)	14.524(3)	11.087(2)
<i>b</i> /Å	39.260(5)	18.742(4)	13.110(3)	10.862(2)	16.183(3)	14.193(3)
<i>c</i> /Å	12.614(2)	20.965(4)	15.374(3)	30.584(6)	18.869(4)	16.251(3)
α /°	90	90	93.67(3)	90	90	108.76(3)
β /°	106.48(4)	94.46(3)	93.94(3)	90	108.97(3)	99.61(3)
γ /°	90	90	91.84(3)	90	90	110.85(3)
<i>V</i> /Å ³	5035.5(14)	3172.5(11)	2585.6(9)	2792.7(10)	4194.0(14)	2145.3(7)
<i>Z</i>	4	4	2	4	4	2
Temperature/K	153(2)	153(2)	163(2)	158(2)	163(2)	161(2)
Fwt/g mol ⁻¹	1399.89	953.63	1493.55	908.90	1192.71	854.26
<i>D</i> _c /Mg m ⁻³	1.847	1.997	1.918	2.162	1.889	1.735
μ /mm ⁻¹	4.367	5.857	4.005	6.403	5.218	2.265
Reflections collected	26 762	23 387	23 669	15 770	27 203	16 481
Unique reflections	8712 (<i>R</i> _{int} = 0.0355)	5650 (<i>R</i> _{int} = 0.0427)	10 830 (<i>R</i> _{int} = 0.0350)	4908 (<i>R</i> _{int} = 0.0682)	7405 (<i>R</i> _{int} = 0.1010)	7603 (<i>R</i> _{int} = 0.0215)
Max., min. transmission	0.5800, 0.2386	0.3590, 0.1220	0.4670, 0.3951	0.7402, 0.3332	0.7448, 0.2125	0.7728, 0.4426
Data, restraints, parameters	8712/0/633	5650/0/398	10 830/0/634	4908/0/334	7405/0/497	7603/0/507
<i>R</i> ₁ , <i>wR</i> ₂ (<i>I</i> > 2σ(<i>I</i>))	0.0504, 0.1011	0.0304, 0.0688	0.0341, 0.0729	0.0399, 0.0769	0.0816, 0.1696	0.0430, 0.1031
<i>R</i> ₁ , <i>wR</i> ₂ (all data)	0.0710, 0.1111	0.0333, 0.0709	0.0406, 0.0773	0.0453, 0.0804	0.0950, 0.1794	0.0507, 0.1117
Goodness-of-fit (<i>F</i> ²)	1.116	1.130	1.083	1.077	1.097	1.077
Largest diff. peak, hole/e Å ⁻³	2.550, -1.707	1.587, -1.479	2.626, -1.356	1.670, -1.584	2.135, -2.024	1.408, -0.789

but had noted difficulties in preparing the former in its pure form.²⁵ However, the Pd(II) [9]aneS₃ complex with dpae, as well as its Pt analogue, was readily prepared, a consequence of the bidentate nature of the ligand. We also attempted to prepare both the bis and mono chloro complexes with the heaviest group 15 analogue, BiPh₃, but no isolable products involving the ligand were obtained. The reactivity we observe with the bismuthine ligand is consistent with prior reports describing its complexation behavior.^{1,5,29}

X-Ray structures†

A summary of data collection and refinement for all six of the structures in this report is presented in Table 1. A summary of key bond distances, M–S_{ax} distances, and bond angles for the coordination sphere is found in Tables 2 and 3. Fig. 1–6 show the thermal ellipsoid perspectives for the cations in complexes 1–6, respectively. With the notable exceptions of the two bis complexes, [Pt([9]aneS₃)(AsPh₃)₂](PF₆)₂ and [Pt([9]aneS₃)(SbPh₃)₂](PF₆)₂ (see further discussion below), the other four complexes form structures best described as elongated square pyramids. This is due to the preferred endodentate conformation of the uncomplexed [9]aneS₃ ligand. As has been observed in virtually all Pt(II) and Pd(II) complexes of [9]aneS₃, the trithiacrown exhibits an axial M–S interaction that is longer than a formal bond, but less than van der Waals contact (3.5 Å for Pt(II), 3.6 Å for Pd(II)).³⁰ We particularly focused on how the metal–sulfur axial interactions change as a function of the group 15 donor ligand, as well

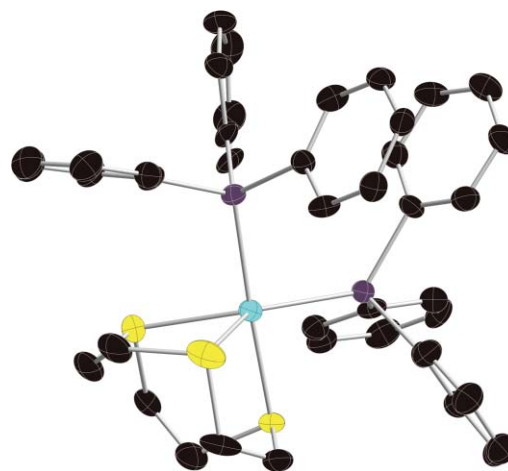


Fig. 1 Thermal ellipsoid perspective of cation in [Pt([9]aneS₃)(AsPh₃)₂](PF₆)₂·2CH₃NO₂ (**1**). (50% probability, H atoms omitted for clarity).

as the interplay between the equatorial sulfur bonds and the corresponding axial interactions. For the six structures presented in the report, all metal–sulfur distances fall within the range of those previously observed for [9]aneS₃ complexes with Pt(II) and Pd(II).

The common structural motif for [9]aneS₃ in its heteroleptic Pt(II) and Pd(II) complexes is an elongated square pyramidal

Table 2 Selected structural features for the reported complexes; included are selected bond lengths (Å),^a bond angles (°),^a τ parameter,^b distances between centroids for the phenyl planes, and angles between phenyl planes for [Pt([9]aneS₃)(AsPh₃)₂](PF₆)₂·2CH₃NO₂ (**1**), [Pt([9]aneS₃)(AsPh₃)(Cl)](PF₆)₂·1.5CH₃NO₂ (**2**), [Pt([9]aneS₃)(SbPh₃)₂](PF₆)₂·2CH₃NO₂ (**3**), [Pt([9]aneS₃)(SbPh₃)(Cl)](PF₆)₂ (**4**), [Pt([9]aneS₃)(dpae)](PF₆)₂·CH₃CN (**5**), and [Pd([9]aneS₃)(dpae)](PF₆)₂·(CH₃)₂CO (**6**)

Parameter	1	2	3	4	5	6
M–S _{eq}	2.321(2)	2.246(1)	2.320(1)	2.255(2)	2.324(3)	2.3574(12)
	2.458(2)	2.315(1)	2.450(1)	2.363(2)	2.333(4)	2.3607(14)
M–S _{ax} ^b	2.584(2)	3.043(6)	2.514(1)	2.787(2)	2.675(4)	2.6737(16)
M–E	2.3907(9)	2.3829(6)	2.5486(9)	2.5304(7)	2.3702(14)	2.3686(11)
	2.3926(9)		2.5447(8)		2.3849(14)	2.3847(8)
Pt–Cl	N/A	2.330(1)	N/A	2.343(2)	N/A	N/A
S _{eq} –M–S _{eq}	87.82(7)	89.86(4)	88.43(4)	88.79(9)	88.79(13)	89.39(5)
E–M–E	93.37(3)	N/A	90.65(2)	N/A	85.16(8)	83.05(4)
E–Pt–Cl	N/A	87.34(3)	N/A	87.06(6)	N/A	N/A
C–E–C	104.0	104.9	102.9	101.2	105.1	107.6
τ^c	0.58	0.14	0.57	0.30	0.16	0.04
Centroid distance	3.84	N/A	3.91	N/A	N/A	N/A
Angles between Ph planes	7.6	N/A	0.60	N/A	N/A	N/A

^a Estimated standard deviations are given in parentheses, E = As or Sb. M = Pt or Pd. ^b For comparative purposes among all [9]aneS₃ Pt(II) and Pd(II) structures, we have consistently defined the axial sulfur in the context of the square pyramidal geometry. In that case, the axial metal–sulfur distance is the longest of the three. However, in the distorted trigonal bipyramidal structures of **1** and **3**, the axial sulfur position will be different since it represents the longest S–Pt–E bond angle. The Pt–S axial distances in that context are 2.321(2) Å in **1** and 2.320(1) Å in **3**. ^c For a square pyramidal structure $\tau = 0$, for a trigonal bipyramidal structure $\tau = 1$; see ref. 31 for additional information.

Table 3 Selected structural features for related literature Pt(II) and Pd(II) [9]aneS₃ complexes; included are metal–sulfur equatorial and axial distances (Å) τ parameter, distances between centroids for phenyl planes, and angles between phenyl planes

Parameter	[Pt([9]aneS ₃)- (PPh ₃) ₂](PF ₆) ₂	[Pt([9]aneS ₃)- (PPh ₃)Cl](PF ₆) ₂	[Pt([9]aneS ₃)- (dppe)](PF ₆) ₂	[Pd([9]aneS ₃)- (AsPh ₃) ₂](PF ₆) ₂	[Pd([9]aneS ₃)- (AsPh ₃)Cl](PF ₆) ₂	[Pd([9]aneS ₃)- (PPh ₃) ₂](PF ₆) ₂
M–S _{eq}	2.3258(2)	2.2609(9)	2.366(2)	2.351(2)	2.262(2)	2.376(3)
	2.485(3)	2.3365(8)	2.369(2)	2.388(2)	2.333(2)	2.406(3)
M–S _{ax} ^b	2.638(3)	3.0778(8)	2.737(2)	2.751(2)	3.094(2)	2.877(3)
τ^b	0.58	0.07	0.01	0.24	0.08	0.27
Centroid distance	3.79	N/A	N/A	3.75	N/A	4.14
Angles between Ph planes	8.8	N/A	N/A	12.9	N/A	24.0
Reference	20	22	23	25	25	19

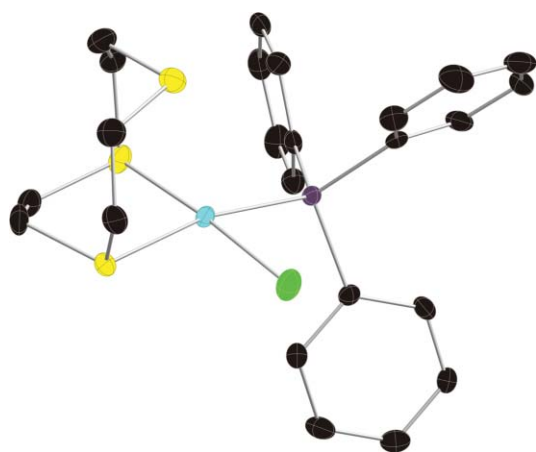


Fig. 2 Thermal ellipsoid perspective of cation in [Pt([9]aneS₃)-(AsPh₃)₂(Cl)](PF₆)₂·1.5CH₃NO₂ (**2**). (50% probability, H atoms omitted for clarity).

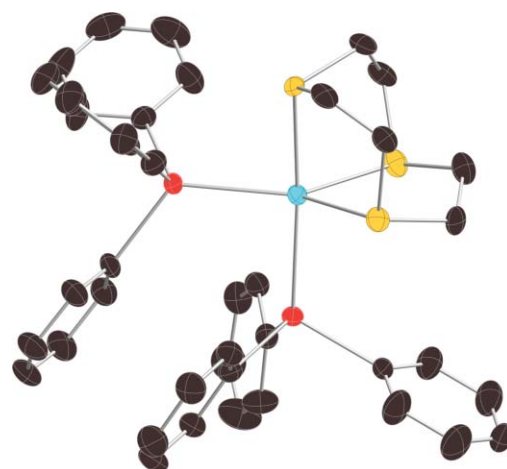


Fig. 3 Thermal ellipsoid perspective of cation in [Pt([9]aneS₃)(SbPh₃)₂](PF₆)₂·2CH₃NO₂ (**3**). (50% probability, H atoms omitted for clarity).

structure with a S₂X₂ + S₁ coordination environment (X = ancillary ligand donor atom). The geometry has now been observed in over 60 [9]aneS₃ complexes with the two group 10 metals. In

contrast, both bis complexes reported here (compounds **1** and **3**) show structures that are highly distorted towards trigonal bipyramid geometry. We had noted a similar distortion in our previously

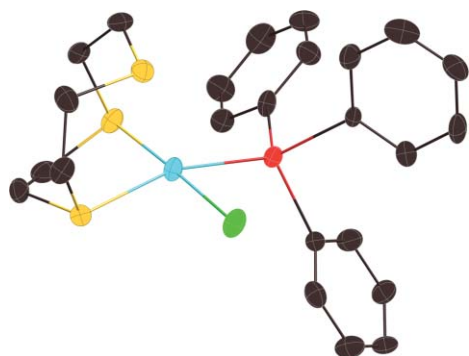


Fig. 4 Thermal ellipsoid perspective of cation in $[\text{Pt}([9]\text{aneS}_3)\text{-(SbPh}_3\text{)(Cl)](PF}_6\text{)}$ (**4**). (50% probability, H atoms omitted for clarity).

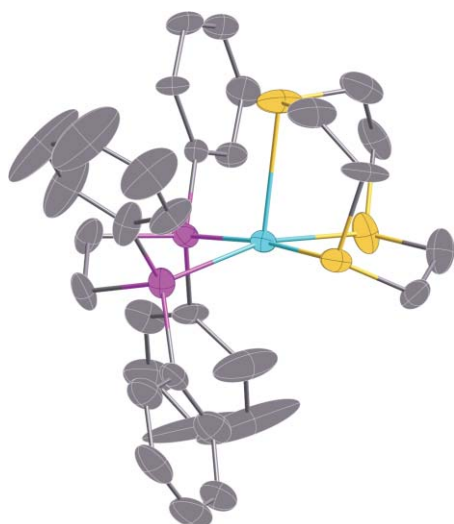


Fig. 5 Thermal ellipsoid perspective of cation in $[\text{Pt}([9]\text{aneS}_3)\text{-(dpae)](PF}_6\text{)}\cdot\text{CH}_3\text{CN}$ (**5**). (50% probability, H atoms omitted for clarity).

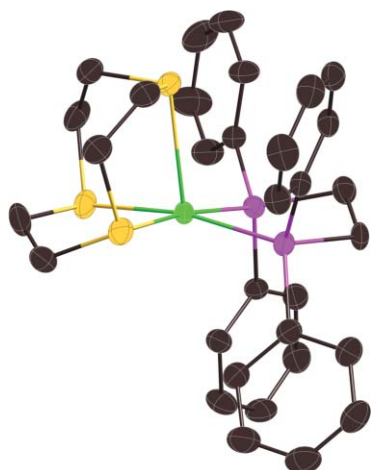


Fig. 6 Thermal ellipsoid perspective of cation in $[\text{Pd}([9]\text{aneS}_3)\text{-(dpae)](PF}_6\text{)}_2\cdot(\text{CH}_3\text{)}_2\text{CO}$ (**6**). (50% probability, H atoms omitted for clarity).

reported $[\text{Pt}([9]\text{aneS}_3)(\text{PPh}_3)_2](\text{PF}_6)_2$ structure.²⁰ The continuum between a square pyramidal geometry and a trigonal bipyramid is conveniently represented by the parameter τ , developed by Reedjik, Addison, and coworkers.³¹ The value of the τ parameter is

0 for an ideal square pyramid and 1 for an ideal trigonal bipyramid. The τ values for the six compounds reported here as well as some pertinent literature compounds are presented in Tables 2 and 3, respectively. The distortion towards trigonal bipyramid geometry can clearly be seen for all three bis EPh_3 ($\text{E} =$ group 15 donor) $\text{Pt}(\text{II})$ $[\text{9}]\text{aneS}_3$ complexes. The degree of distortion among the three complexes is essentially identical despite the differences in the nature of the group 15 donor atom (0.58).§ Our observation implies that the distortion towards a trigonal bipyramidal shape is not a function of the identity of the ligand donor, but rather lies in another factor.

We propose that the effect originates with intramolecular π – π interactions between phenyl groups on two different monodentate triphenylpnictogen ligands. In support of this hypothesis, we note that none of the mono chloro $\text{Pt}(\text{II})$ complexes involving EPh_3 ligands show this large degree of trigonal bipyramidal distortion nor do the analogous $\text{Pd}(\text{II})$ $[\text{9}]\text{aneS}_3$ complexes which contain two EPh_3 ligands. Thus, the distortion requires the presence of a $\text{Pt}(\text{II})$ center along with two group 15 donor ligands bearing a phenyl group. If either of these conditions are not met, the $[\text{9}]\text{aneS}_3$ complex shows the anticipated and common elongated square pyramidal motif. Also, there are no close contacts that arise from solvent, anion or packing effects that are unique to the $\text{Pt}(\text{II})$ complexes that could result in the structural distortion. Our group has previously noted three distinct types of intermolecular π – π stacking interactions between diimine ligands in $\text{Pt}(\text{II})$ and $\text{Pd}(\text{II})$ $[\text{9}]\text{aneS}_3$ complexes.¹¹ Furthermore, the importance of intermolecular and intramolecular interactions involving phenyl rings in $[\text{PPh}_3]_4^+$ structures, termed “phenyl embraces”, has been highlighted in crystal engineering work by Dance and Scudder.^{32,33} They had also noted similar interactions between phenyl groups in arsenic analogues.³⁴ We identify the presence of intramolecular π – π interactions between phenyl groups in the bis group 15 EPh_3 , $\text{Pt}(\text{II})$ complexes, including importantly the triphenylstibine complex. The phenyl interactions that we observe are an offset face-to-face interaction, rather than an edge-to-face interaction, and are shown in Fig. 7 for the bis SbPh_3 complex.³² The calculated distances between the two centroids for the interacting phenyl rings are presented in Table 2. It should be noted that complexes which show the distortion towards a trigonal bipyramidal geometry all possess two common structural features; phenyl ring centroid distances in the 3.79–3.91 Å range and relatively small angles ($< 10^\circ$) between the mean least squares planes between the two phenyl rings.

Interestingly, the $\text{Pd}(\text{II})$ $[\text{9}]\text{aneS}_3$ complexes with two PPh_3 or AsPh_3 ligands do not show the trigonal bipyramidal distortion to the same degree as the analogous $\text{Pt}(\text{II})$ complexes. The bis triphenylphosphine $\text{Pd}(\text{II})$ complex has a large distance between its phenyl rings (> 4.0 Å).¹⁹ While the bis triphenylarsine has a short centroid distance (3.75 Å), its two phenyl rings are turned away from a parallel position as the angle between the mean least-squares planes for the phenyl groups is 12.9° which diminishes the π – π interactions between the rings.²⁵ The PPh_3 complex similarly

§ Excluding the three bis EPh_3 complexes discussed here, the median value of τ for all heteroleptic $\text{Pt}(\text{II})$ $[\text{9}]\text{aneS}_3$ structures (41 total) is 0.05. Accordingly, the elongated square pyramidal shape is seen much more commonly. Examining data for $\text{Pd}(\text{II})$ $[\text{9}]\text{aneS}_3$ structures, excluding the bis AsPh_3 and PPh_3 complexes, the median value of τ for the other seventeen heteroleptic $\text{Pd}(\text{II})$ $[\text{9}]\text{aneS}_3$ structures is also 0.05.

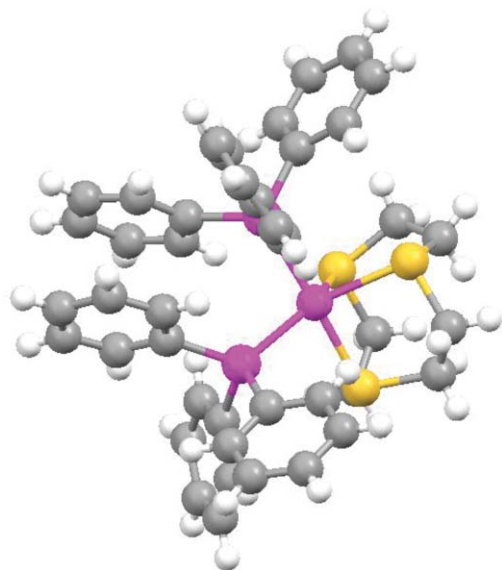


Fig. 7 Intramolecular π - π interaction between phenyl rings in $[\text{Pt}(\text{[9]aneS}_3)(\text{AsPh}_3)_2](\text{PF}_6)_2 \cdot 2\text{CH}_3\text{NO}_2$ (**1**). The distance between centroids for the two phenyl rings is 3.84 Å.

has a large angle between the mean least-squares planes for its phenyl groups (24.0°). We would underscore, however, that these two Pd(II) complexes are also the ones that exhibit the greatest distortion towards trigonal bipyramidal geometry out of any of the reported structures for Pd(II) complexes with [9]aneS₃ ligands (τ values of 0.24 (As complex) and 0.27 (P complex)).³⁵

Other distinctive structural features found in the two bis complexes, in addition to the distortion towards a trigonal bipyramidal shape, are their very short Pt–S axial distances (Pt–S = 2.584(2) Å for bis AsPh₃ complex; Pt–S = 2.514(1) Å for bis SbPh₃ complex). Indeed, these are the two shortest axial sulfur distances yet observed in all reported Pt(II) [9]aneS₃ crystal structures. As seen in Table 2, there is a notable periodic trend with the axial Pt–S distances shortening as the group 15 donor changes in the order, P > As > Sb. We believe that the increasingly poorer donor qualities of the larger pnictogen ligand are responsible for the sequence. In earlier papers, we have highlighted the reciprocal relationship that Pt(II) and Pd(II) [9]aneS₃ complexes with shorter M–S axial distances show longer equatorial bonds and *vice versa*.⁹ The six complexes in this report continue to demonstrate the correlation. In addition, we have previously underscored another important structural feature to monitor [9]aneS₃ complexes, the sum of the three metal–sulfur distances. Like the axial sulfur lengths, the sum of the three metal–sulfur distances also shortens with the change in the group 15 donor. Both the bis AsPh₃ and bis SbPh₃ complexes show the shortest M–S distance sum of any of the Pt [9]aneS₃ structures reported. As such, these two Pt(II) complexes approach true five-coordination more than any of the prior complexes involving the [9]aneS₃ ligand.¶ The tendency for larger pnictogen donors like Sb to favor

five-coordinate complexes has been noted from the infancy of its complexation chemistry, and our data support that conception.³⁶ The ability of certain ligands to reduce electron density on a metal center through their π acidity has been cited as a factor favoring trigonal pyramidal five-coordination.³⁷ Our results suggest that the same effect can also be achieved by employing a poor σ donor ligand. As the group 15 family donor is changed from P to As to Sb, the [9]aneS₃ ligand clamps down harder on the metal ion *via* all three sulfurs to compensate for the increasingly poorer donor qualities of the ancillary ligand.

The same trend discussed above for the bis pnictogen complexes is similarly observed in the three related chloro complexes of Pt(II) with [9]aneS₃. That is, the axial Pt–S distances shorten as you descend the group 15 family, P > As > Sb (P = 3.08 Å, As = 3.04 Å, Sb = 2.79 Å). We had reported the same trend in the related Pd(II) [9]aneS₃ chloro complexes with group 15 donors.²⁵ The two new chloro complexes form elongated square pyramidal geometries around the Pt center with the anticipated *cis*-[S₂ECl + S₁] (E = group 15 donor) coordination environment. The two *cis* donors from the [9]aneS₃ ligand, the group 15 donor, and chloride form the square planar base of the pyramid. In complex **2**, the Pt(II) ion is raised 0.156 Å above the mean square basal plane defined by the S₂AsCl donor set and directed towards the axial sulfur (S1). Similarly, complex **4** shows the Pt(II) ion is raised above the mean square plane of the S₂SbCl donor set, but to a larger degree, 0.230 Å. In contrast to the bis EPh₃ complexes, the chloro complexes do show a periodic trend for the distortion from an ideal square pyramidal shape, with the Sb complex displaying the largest τ value (Sb > As > P; τ = 0.30, 0.14, 0.07, respectively).

The better *trans* directing chloro ligand results in a shorter Pt–S equatorial bond *trans* to it as compared to the bond *trans* to the As or Sb donor. The effect results in the Pt–S equatorial bond *trans* to the chloro ligand almost 0.02 Å shorter in the arsine complex, but over 0.1 Å shorter in the stibine complex. We believe that the relative poorer donor qualities of the Sb ligand are responsible for the shorter bond length as well as the greater distortions towards trigonal bipyramidal geometry in the complex. We also note that the equatorial Pt–S distances are shorter in the chloro-EPh₃ complexes than for the analogous bis EPh₃ complexes due to the presence of the π -donating chloro ligand. The trend in the difference between the longer Pt–S equatorial bond lengths in the [Pt([9]aneS₃)(EPh₃)₂]²⁺ complexes and the shorter Pt–S bonds in the [Pt([9]aneS₃)(EPh₃)(Cl)]⁺ complexes follows the periodicity of group 15 with a respective change of 0.13, 0.10, and 0.08 Å in the order of P, As, and Sb. The longer axial Pt–S distances in the two chloro complexes are balanced with the previously noted shorter Pt–S equatorial bonds. For the three chloro complexes with EPh₃ ligands, their axial Pt–S distances fall intermediate between the bis EPh₃ complexes and [Pt([9]aneS₃)Cl₂] (As: 2.58, 3.04, 3.26 Å; Sb: 2.51, 2.79, 3.26; P: 2.64, 3.08, 3.26 Å), gradually lengthening as chlorides successively replace pnictogen donors in the coordination sphere. The axial sulfur (S1) is also angled away from the pnictogen ligand and directed towards the sulfur *trans* to the chloride (S7) (for AsPh₃ complex; S₁–Pt–S₄ = 83.54(7)°; S₁–Pt–S₇ = 79.24(7)°; for SbPh₃ complex; S₁–Pt–S₄ = 86.94(7)°; S₁–Pt–S₇ = 83.40(7)°). Among the three chloro EPh₃ complexes with Pt(II), the Pt–Cl bond lengths show surprisingly little change (2.33–2.34 Å), particularly given the large differences in Pt–S bonds. The observation suggests that the Pt–Cl bond length is

¶ The difference between the shortest and longest Pt–S distances are 0.28, 0.26, and 0.19 Å respectively for the 2 × PPh₃, AsPh₃, and SbPh₃ complexes. These values contrast the median difference of 0.64 Å between the longest and shortest Pt–S distances in all other Pt(II) [9]aneS₃ structures, illustrating how the group 15 donor is effecting the trend towards true five-coordination.

largely affected by the *trans* thioether sulfur with little contribution from the *cis* pnictogen donor. Due to the better π donating chloro ligand, the *trans* Pt–S bond is always the shorter of the two bonds, illustrating both the sensitivity and ability of the coordinated [9]aneS₃ ligand to adapt to changes in the donor/acceptor properties of whatever ancillary ligand that might be present. Thus, Pt(II) and Pd(II) complexes with [9]aneS₃ are useful structural probes for examining complexation behaviors in a wide range of ancillary ligand types.

The Pt(II) and Pd(II) complexes with the chelating dpae ligand exhibit the anticipated square pyramidal geometry. In the Pt(II) complex with dpae, the Pt ion is raised 0.220 Å above the mean least-squares plane defined by the S₂As₂ donor set and directed towards the axial sulfur. The Pd(II) is also raised out of the S₂As₂ plane towards S1, but to a smaller degree, 0.178 Å. It is interesting to note that the [Pd([9]aneS₃)(dpae)]²⁺ complex has the shortest known axial Pd–S distance in any of the twenty-four structures of this type; a consequence of two As donors. Similarly, for the Pt(II) dpae analog only the previously discussed bis SbPh₃ and AsPh₃ complexes (out of all forty-seven Pt(II) structures) have shorter axial Pt–S distances. Also, both complexes have a three M–S bond sum that is very short with the Pd(II) dpae complex being the shortest among Pd(II) [9]aneS₃ structures. For the Pt(II) dpae complex, it has the smallest sum of Pt–S distances for any complex except for the bis SbPh₃ complex. We note the ability of the trithiacrown ligand to adjust its coordination mode, due to the poorer σ donor abilities of the group 15 donor, regardless of the denticity of the pnictogen ligand. There is a reduction in charge on the metal due to the poor sigma donor qualities of the ligand and similar effects have been observed with Pt(II) [9]aneS₃ complexes containing π -acid ligands.^{9,10,18} Importantly, we would stress that neither of the two dpae complexes shows much distortion towards a trigonal bipyramid geometry, illustrating that the poor donor properties of the pnictogen alone cannot be responsible for that distortion ($\tau = 0.16$ (Pt) and 0.080 (Pd)).

In prior publications involving [9]aneS₃ complexes, the Pd(II) complexes showed shorter axial metal–sulfur distances, on average about 0.1 Å compared to analogous Pt(II) complexes.^{12,18} However, for comparisons of the Pt(II) and Pd(II) complexes in this report, no general trend emerges with regards to any of the metal–sulfur distances. We would note that for the two sets of bis EPh₃ (E = P and As) complexes, the Pd(II) complexes show the shorter equatorial bond distances, but the Pt(II) complexes display shorter axial lengths and a shorter sum of the three metal–sulfur distances, possibly due to the trigonal bipyramidal distortion. In comparing analogous Pt(II) and Pd(II) [9]aneS₃ complexes with identical ancillary group 15 donor ligands, the Pt(II) complex always shows the greater distortion towards a trigonal bipyramidal geometry. As typically observed in transition metal complexes with EPh₃ complexes, the C–E–C angles for the phenyl rings are compressed (see Table 2), and the degree of compression increases periodically with the larger group 15 donor.^{1–3} In contrast to the anticipated period trend, the E–Pt–E angles actually decrease with the larger group 15 donor (P = 95.6°, As = 93.4°, Sb = 90.7°). The source for the trend is not the trigonal bipyramidal distortion as the related chloro complexes also follow the same pattern in their Cl–Pt–X angles, with the antimony complex again showing the smallest bite angle around the platinum centre. The Pt–As and Pt–Sb bond lengths for all five [9]aneS₃ complexes are in the range

previously observed for these types of bonds.^{39–41} However, the Pt–E distance does decrease as thioether sulfur donors are replaced by halide donors such that [Pt(EPh₃)₂X₂] (X = Cl or Br) exhibit shorter metal–pnictogen distances than the Pt thioether complexes presented here.^{38–40}

The relative *trans* influence of pnictogen ligands has seen considerable discussion in the literature.³⁸ In our thiocrown complexes involving As and P donors, the Pt–S bond that is *trans* to the pnictogen donor always shows the shortest bond when E is an arsenic donor and longest with a phosphorus ligand. The same sequence is seen for the two bis EPh₃ complexes, the two bidentate dppe and dpae complexes, and both mono chloro complexes. In the latter complexes, the Pt–S bonds *trans* to the chloro ligand are always shorter than any of the pnictogens, suggesting an ordering of *trans* influence among the three donor types of P > As > Cl[–]. We propose that the ordering is reflective of the ability of the ligand to function as a σ donor. The positioning of the SbPh₃ ligand among the group 15 donor series is difficult. For the chloro complex, the Pt–S *trans* bond to SbPh₃ is the longest among the three pnictogen complexes, but in the bis complex it is the shortest. The noted distortions towards trigonal bipyramidal geometry could strongly affect the *trans* influence, making a definitive assignment of the relative position of SbPh₃ in the series of group 15 ligands difficult.

We would like to highlight two aspects of these π – π intramolecular interactions that are unique to this report. For the first time, π – π intramolecular interactions in a bis AsPh₃ complex as well as for an analogous SbPh₃ complex are noted. A survey of the Cambridge Structural Database (CSD) shows 128 bis AsPh₃ complexes with any transition metal, of which only 6 show this interaction.³⁵ Similarly, out of 82 bis SbPh₃ complexes structurally characterized with any transition metal, we have found only a single example of intramolecular π – π interactions between phenyl rings.^{35**} There are a decreasing number of examples of intramolecular π – π interactions in EPh₃ complexes (both actual numbers and proportionally) with the larger group 15 donor. This is due to a larger number of *trans* complexes with the ligands as well as larger E–M–E angles which minimize the approach of the two phenyl substituents. To our knowledge, there have been no literature reports of this type of interaction influencing the stereochemistry of a metal complex and distorting it towards a trigonal bipyramidal shape. Accordingly, we feel that this is a rare example of a π – π intramolecular interaction significantly influencing the stereochemistry at a metal center.

|| A search of the CSD for all transition metal complexes containing at least two AsPh₃ ligands reveals 128 structures.³⁵ We examined all of these complexes to find structural features similar to the ones presented here. Out of these, we have identified only six that have both centroid distances less than 4.0 Å and a mean least squares plane angle of 10.0° or less. All involve Pt(II) (five examples) or Pd(II) centers containing ligands with strongly electron-withdrawing substituents. We do not mean imply that these values are defining structural features for an intramolecular π – π interaction, but the relatively few examples serve to illustrate how uncommon are our reported structural features. Also, we would note that the interactions do not appear to have been discussed in the prior structures.

** A similar search of the CSD for all metal complexes containing at least two SbPh₃ reveals 82 structures.³⁵ We have followed the search parameters described above and found only a single example (JUJUL) that showed the described structural features.

Table 4 Comparative data for ^{195}Pt NMR and visible spectroscopies

Complex ^a	^{195}Pt NMR δ ($\nu_{1/2}$)	λ_{max} /nm d–d trans.	Ref.
$[\text{Pt}(\text{[9]aneS}_3)(\text{AsPh}_3)_2]^{2+}$ (1)	–4489, <i>s</i> (120Hz)	434	This work
$[\text{Pt}(\text{[9]aneS}_3)(\text{AsPh}_3)(\text{Cl})]^+$ (2)	— ^b	413	This work
$[\text{Pt}(\text{[9]aneS}_3)(\text{SbPh}_3)_2]^{2+}$ (3)	–4822, <i>s</i> (640Hz)	454	This work
$[\text{Pt}(\text{[9]aneS}_3)(\text{SbPh}_3)(\text{Cl})]^+$ (4)	— ^b	437	This work
$[\text{Pt}(\text{[9]aneS}_3)(\text{dpae})]^{2+}$ (5)	–4772, <i>s</i> , (140Hz)	415	This work
$[\text{Pd}(\text{[9]aneS}_3)(\text{dpae})]^{2+}$ (6)	N/A	466	This work
$[\text{Pt}(\text{[9]aneS}_3)(\text{PPh}_3)_2]^{2+}$	–4399, <i>t</i> , (49Hz)	— ^b	20
$[\text{Pt}(\text{[9]aneS}_3)(\text{PPh}_3)(\text{Cl})]^+$	–4080, <i>d</i> , (70Hz)	— ^b	22
$[\text{Pt}(\text{[9]aneS}_3)(\text{dppe})]^{2+}$ ^c	–4069, <i>t</i> , (41Hz)	— ^b	23

^a All cationic complexes are reported as PF_6^- salts exclusively to minimize anion effects. ^b Not observed. ^c dppe = 1,2-bis(diphenylphosphino)ethane

NMR spectroscopy

In the proton NMR spectra for complexes **1**, **3**, **5**, and **6**, the twelve methylene protons of the [9]aneS₃ appear as a symmetrical multiplet with a distinctive AA'BB' splitting pattern observed in virtually all of its Pt(II) and Pd(II) complexes.^{12,20} In contrast, the two chloro complexes, compounds **2** and **4**, show a broad multiplet for the [9]aneS₃ (see ESI†). For the Pt(II) complex with dpae (compound **5**), we observe $^3J_{\text{H-}^{195}\text{Pt}}$ coupling in its ^1H NMR spectrum for the ligand's methylene resonances which results in ^{195}Pt satellites. We see similar carbon–platinum coupling in the same complex for three of the carbon atoms (dpae methylene carbons, *ortho* ring carbons, quaternary ring carbon). The Pt complexes generally show $^2J_{^{13}\text{C-}^{195}\text{Pt}}$ coupling for the quaternary ring carbon atom and $^3J_{^{13}\text{C-}^{195}\text{Pt}}$ coupling for two *ortho* ring carbon atoms which allows for the assignment of all peaks in their ^{13}C NMR spectra. The aromatic region in the proton and ^{13}C NMR spectra for the six group 15 donor complexes is as expected.

Despite the asymmetric nature of the coordination environment found in the chloro complexes, the coordinated [9]aneS₃ ligand always displays a single resonance in its ^{13}C NMR spectra due to the six equivalent methylene carbons which are involved in a rapid fluxional process. We have previously noted a single ^{13}C NMR resonance in other asymmetrical [9]aneS₃ complexes such as ones involving cyclometalating ligands and related chloro complexes.^{18,22} The ^{13}C NMR [9]aneS₃ singlet is always shifted 1–2 ppm downfield in the phosphine complexes compared to the analogous arsine complexes. Surprisingly, the line width for the [9]aneS₃ ^{13}C signal is strongly affected by the identity of the group 15 donor (see ESI†) as the peaks become progressively wider as you descend the family.

As seen in Table 4, there is a clear periodic trend in ^{195}Pt NMR chemical shifts and group 15 donors. The larger group 15 donors result in a progressive upfield chemical shift for the ^{195}Pt nucleus (see ESI for spectra†) for both monodentate and bidentate pnictogen ligands, with the dpae complex shifted 750 ppm upfield relative to the dppe complex. Thus, the ^{195}Pt NMR chemical shift is quite sensitive to the ligand environment around the metal center. Curiously, attempts to acquire ^{195}Pt NMR spectra for the two chloro complexes (complexes **2** and **4**) were unsuccessful despite numerous attempts in concentrated solutions over large chemical shift ranges and acquisition times (several days in some cases)

and our prior NMR experiences with a number of related Pt(II) [9]aneS₃ complexes.^{14,23}

Electronic spectroscopy and electrochemistry

Two main types of electronic transitions are observed for all six complexes, one lower energy and lower intensity transition and at least one additional band of both higher energy and intensity. These two transitions are assigned as d–d transitions and metal-to-ligand charge transfer transitions, respectively. The energy of the d–d transition allows an apt comparison of the ligand field strengths among these ligands, and the data are summarized in Table 4. The antimony donor is a weaker field ligand than the arsenic which is consistent with the anticipated periodic trend for the group 15 donors.⁴¹ That is, the ligand field strength diminishes on the order of P > As > Sb. The stronger field phosphine ligands result in a higher energy d–d band that is then obscured by the more intense MLCT bands. We note that both AsPh₃ or SbPh₃ function as weaker field ligands than chloride since replacement of Cl[–] by either of these group 15 donors results in a weaker ligand field, as seen in a red shift in the absorption of the d–d transition. We also have recently reported similar trends for Pd [9]aneS₃ complexes with AsPh₃.²⁴ As expected, the bidentate dpae ligand is a stronger field ligand than the monodentate AsPh₃. In comparisons between arsine donor ligands, Pt(II) complexes show stronger ligand fields than the analogous Pd(II) complexes as expected based upon the greater ligand interactions with the Pt 5d orbitals.⁴²

We have examined the electrochemistry of the four As complexes using cyclic voltammetry. None of the complexes exhibit oxidative electrochemistry except $[\text{Pt}(\text{[9]aneS}_3)(\text{AsPh}_3)(\text{Cl})]^+$ which shows an irreversible oxidation wave at +626 mV vs. Fc/Fc⁺. This is assigned as a one-electron oxidation of the Pt(II) center, and the oxidation is facilitated by the presence of the anionic chloro ligand in contrast to the other complexes with exclusively neutral ligands. All three Pt(II) complexes show an irreversible reduction wave that is assigned as reduction to Pt(0). The reduction of the dpae complex occurs at a more negative potential than the bis AsPh₃. Also, the reduction potentials for the arsenic complexes occur at more negative reduction potentials than the related phosphine complexes, indicating they are harder to reduce and consistent with the donor properties of the two pnictogen atoms. The Pd(II) dpae complex shows a quasi-reversible wave at –952 mV vs. Fc/Fc⁺ and an irreversible reduction at –1406 mV vs. Fc/Fc⁺. These are assigned as a Pd(II)/Pd(I) and Pd(I)/Pd(0) couples respectively.

Conclusion

In summary, we have synthesized and characterized a new series of heteroleptic platinum(II) complexes containing the thiocrown [9]aneS₃ with monodentate and bidentate group 15 ligands. The increasing poorer donor qualities of the larger pnictogen ligands manifest themselves in the structural and spectroscopic properties of the complex. As expected, the larger pnictogen ligand forms the weaker ligand field. The trithiacrown compensates for poorer donor quality with shorter metal–sulfur bond distances, approaching a pentacoordinate complex with the larger pnictogens. However, the bis triphenylpnictogen complexes display an unusual distortion towards a trigonal bipyramidal geometry which arises from intramolecular π – π interactions between phenyl rings in the two ligands as opposed to the identity of the group 15 donor.

Methods and materials

All solvents and reagents were purchased from Aldrich Chemical Company and used as received. The starting complexes [Pt([9]aneS₃)Cl₂] and its Pd(II) analogue were prepared according to published methods.⁴³ Elemental analyses were performed by Atlantic Microlab, Inc. of Atlanta, GA. Fourier transform IR spectra were obtained as KBr powders using pre-weighed 500 mg packets and a Nicolet Impact 410 spectrometer equipped with an ATR accessory. Ultraviolet-visible spectra were obtained in acetonitrile using a Varian DMS 200 UV-visible spectrophotometer. ¹³C{¹H}, ¹⁹⁵Pt{¹H} and ¹H NMR spectra were recorded on a JEOL ECX-400 NMR spectrometer. Residual solvent peaks were used for both the deuterium lock and reference for ¹³C{¹H} and ¹H NMR spectra while ¹⁹⁵Pt{¹H} NMR spectra were externally referenced to [PtCl₄]²⁻ at –1624 ppm.⁴⁴ Electrochemical measurements were performed using a Bioanalytical Systems CV50W analyzer. The supporting electrolyte was 0.1 M tetra-n-butylammonium tetrafluoroborate in acetonitrile, and sample concentrations were approximately 2 mM. All voltammograms were recorded at a scan rate of 100 mV s⁻¹. The standard three-electrode configuration used is as follows: 1.6 mm diameter Pt disk working electrode, Pt wire auxiliary electrode, and Ag/AgCl reference electrode. All reported potentials were internally referenced to FeCp₂⁺/FeCp₂, which in this solution was found at +0.411 V relative to the reference electrode.

Preparation of complexes

[Pt([9]aneS₃)(AsPh₃)₂](PF₆)₂ (1). A mixture of [Pt([9]aneS₃)Cl₂] (50.0 mg, 0.112 mmol) and AsPh₃ (69.0 mg, 0.225 mmol) were refluxed in CH₃NO₂ (25 mL) for 1 h, producing a clear, orange solution. The arsine ligand dissolved immediately, but the Pt complex slowly went into solution. The reaction was allowed to cool slightly before the addition of solid NH₄PF₆ (37.0 mg, 0.227 mmol), and the solution was refluxed for another 30 min. The reaction was cooled in ice overnight to precipitate colorless crystals of NH₄Cl which were removed *via* filtration from the orange solution. The contents of the reaction flask were concentrated to 2/3 of its original volume. Slow diethyl ether diffusion (1 week) into the concentrated solution produced orange crystals of (1). This was isolated by decantation and rinsed 2 × with 10 mL of diethyl ether. Yield: 0.109 mg, 76.2%. Anal. Found:

C, 39.19; H, 3.50; S, 7.26. C₄₂H₄₂As₂F₁₂P₂PtS₃ requires C, 39.48; H, 3.31; S, 7.53. δ_{H} (400 MHz, CD₃NO₂): 7.60–7.42 (m, 30H, *Ph*), 2.97–2.84, (m, 6H, [9]aneS₃), 2.72–2.58 (m, 6H, [9]aneS₃). δ_{C} (100 MHz, CD₃NO₂): 134.59 (³*J*_{Pt-C} = 13 Hz, 12C, *Ph*), 133.65 (6C, *Ph*), 131.31 (12C, *Ph*), 130.16 (²*J*_{Pt-C} = 42 Hz, 6C, *Ph*), 36.09 (6C, *v*_{1/2} = 3 Hz, [9]aneS₃). δ_{Pt} (85.9 MHz, CD₃NO₂): –4491 (*v*_{1/2} = 120 Hz). UV-Vis (CH₃CN, nm (ϵ /M⁻¹ cm⁻¹)): 434 (2.12 × 10²), 264 (9.8 × 10⁴). *v*_{max}, cm⁻¹: 3074, 3069, 3041, 3000, 2972, 2938, 1559, 1476, 1439, 1290, 1193, 1000, 840 (s, PF₆⁻), 831, 738, 693, 690, 555 (s, PF₆⁻), 545. The complex shows no oxidative electrochemistry, but does show an irreversible reduction wave at –1286 mV *vs.* Fc/Fc⁺.

[Pt([9]aneS₃)(AsPh₃)(Cl)](PF₆) (2). This complex was prepared by means of an identical procedure to (1), but using a single equivalent of AsPh₃. The stoichiometric quantities in this reaction included: [Pt([9]aneS₃)Cl₂] (51.0 mg, 0.114 mmol), AsPh₃ (35.0 mg, 0.114 mmol), and NH₄PF₆ (20 mg, 0.123 mmol). The color of the solution was yellow-orange prior to crystallization. Yield: 46 mg, 42%. Anal. Found: C, 32.18; H, 3.33; S, 10.19; Cl, 3.53. C_{25.5}H_{31.5}AsClF₆N_{1.5}O₃PPtS₃ requires C, 32.11; H, 3.33; S, 10.09; Cl, 3.72. δ_{H} (400 MHz, CD₃NO₂): 7.79–7.58 (m, 15H, *Ph*), 3.19–3.03 (m, 6H, [9]aneS₃). δ_{C} (100 MHz, CD₃NO₂): 135.04 (³*J*_{Pt-C} = 13 Hz, 6C, *Ph*), 133.04 (3C, *Ph*), 130.69, (6C, *Ph*) 130.55 (²*J*_{Pt-C} = 45 Hz, 3C, *Ph*), (37.69–36.86 (broad, 6C, *v*_{1/2} = 29 Hz, [9]aneS₃). We could not detect a ¹⁹⁵Pt NMR peak over a total range between –3000 to –5000 ppm despite obtaining over 20 000 transients (65 h) in a typical run. UV-Vis (CH₃CN, nm (ϵ /M⁻¹ cm⁻¹)): 413 (sh, 9.2 × 10¹), 259 (1.5 × 10⁴). *v*_{max}, cm⁻¹: 3074, 3064, 2970, 2918, 2907, 1555, 1481, 1435, 1372, 1180, 1162, 1080, 1023, 993, 936, 840 (s, PF₆⁻), 746, 737, 693, 655, 553 (s, PF₆⁻). The complex shows an irreversible oxidation wave at +626 mV and an irreversible reduction wave at –1680 mV *vs.* Fc/Fc⁺. There is also a weak irreversible reduction at +76 mV *vs.* Fc/Fc⁺ associated with the oxidation.

[Pt([9]aneS₃)(SbPh₃)₂](PF₆)₂ (3). A mixture of [Pt([9]aneS₃)Cl₂] (50.0 mg, 0.112 mmol) and SbPh₃ (159 mg, 0.450 mmol) were refluxed in 50 mL of CHCl₃:CH₃NO₂ (1:1) solvent for 1 h. The stibine ligand quickly dissolved albeit the Pt complex slowly went into solution. The flask was cooled slightly before the addition of NH₄PF₆ (37 mg, 0.23 mmol) which resulted in a turbid, peach-colored solution. The solution was refluxed for an additional 30 min. At this point, a clear orange-yellow solution was present. Cooling overnight at 0° precipitated colorless crystals of NH₄Cl which were removed by filtration. The filtrate was concentrated to 2/3 of its original volume, and three drops of CHCl₃ were added to facilitate solubility. Slow diffusion (1 week) of diethyl ether into the concentrate produced orange crystals. The clear, colorless supernatant solution was decanted, and the orange crystals rinsed twice with 10 mL of diethyl ether. A yield of 71.0 mg (22.8%) of 3 were recovered. Anal. Found: C, 36.32; H, 3.27; S, 6.59. C₄₂H₄₄F₁₂OP₂PtS₃Sb₂ requires C, 36.31; H, 3.19; S, 6.92. δ_{H} (400 MHz, CD₃NO₂): 7.54–7.45 (m, 30H, *Ph*), 2.99–2.94 (m, 6H, [9]aneS₃). δ_{C} (100 MHz, CD₃NO₂): 136.68 (12 C, *Ph*), 133.62 (6 C, *Ph*), 131.67 (12C, *Ph*), 126.93 (²*J*_{Pt-C} = 56 Hz, 6C, *Ph*), 37.54 (broad, 6C, *v*_{1/2} = 3 Hz, [9]aneS₃). δ_{Pt} (85.9 MHz, CD₃NO₂): –4822 (*v*_{1/2} = 640 Hz). UV-Vis (CH₃CN, nm (ϵ /M⁻¹ cm⁻¹)): 454 (273), 287 (2.55 × 10⁴), 265 (9.07 × 10³). *v*_{max}, cm⁻¹: 3085, 3074, 3023, 2958, 2944, 1475, 1432, 1064, 996, 840 (s, PF₆⁻), 747, 685, 668, 560 (s, PF₆⁻). We also note that yellow

needles of a second crystalline material were present causing the low yield of **3**. These needles have been identified as the compound $[\text{Pt}(\text{[9]aneS}_3)(\text{SbPh}_3)(\text{Ph})](\text{PF}_6)$.⁴⁵

[Pt([9]aneS₃)(SbPh₃)(Cl)](PF₆) (4). This complex was prepared by a procedure similar to (**3**) except one equivalent of SbPh₃ was used. The following stoichiometric quantities were employed in the reaction: $[\text{Pt}(\text{[9]aneS}_3)\text{Cl}_2]$ (50.0 mg, 0.112 mmol); SbPh₃ (38.0 mg, 0.108 mmol) and NH₄PF₆ (20.0 mg, 0.123 mmol). Following the reflux, the color of the solution was a turbid orange. Cooling overnight produced colorless crystals of NH₄Cl which were removed by filtration. The filtrate was concentrated to 2/3 of its original volume. Three drops of CHCl₃ were added to facilitate solubility, and diethyl ether slowly (1 week) diffused into the solution. Red crystals of **4** were produced. The supernatant was removed by decantation, and the crystals rinsed twice with 10 mL of diethyl ether. A yield of 81.0 mg (82.5%) of **4** was obtained. Anal. Found: C, 31.05; H, 3.06; S, 10.58. C₂₄H₂₇F₆PClPtS₃Sb requires: C, 31.09; H, 3.15; S, 10.38. δ_{H} (400 MHz, CD₃NO₂): 7.77–7.75 (m, 6H, *Ph*), 7.65–7.54 (m, 9H, *Ph*), 3.27–3.00 (m, 6H, [9]aneS₃). δ_{C} (100 MHz, CD₃NO₂): 137.21 (6C, *Ph*), 133.00 (3C, *Ph*), 131.17 (6C, *Ph*), 127.99 (3C, *Ph*), 37.60–36.22 (very broad, 6C, $\nu_{1/2}$ = 110 Hz, [9]aneS₃). We could not detect a ¹⁹⁵Pt NMR peak over a total range between –3000 to –5000 ppm despite obtaining over 20 000 transients (65 h) in a typical run. UV-Vis (CH₃CN, nm ($\epsilon/\text{M}^{-1}\text{cm}^{-1}$)): 437(161), 265(1.74 × 10⁴). ν_{max} , cm⁻¹: 3068, 3051, 3012, 2972, 2887, 2867, 1478, 1430, 1410, 1302, 1186, 1138, 1059, 1019, 835 (s, PF₆⁻), 732, 689, 665, 551 (s, PF₆⁻).

[Pt([9]aneS₃)(dpae)](PF₆)₂ (5)

The compound was prepared by a procedure identical to compound (**1**). The following stoichiometric quantities were used: $[\text{Pt}(\text{[9]aneS}_3)\text{Cl}_2]$ (50.0 mg, 0.112 mmol), 1,2-bis(diphenylarsenio)ethane (dpae) (55.0 mg, 0.113 mmol), and NH₄PF₆ (37.0 mg, 0.227 mmol). Ether diffusion into a concentrated deep-yellow CH₃NO₂ solution produced yellow needle-like crystals. The crystals were collected, washing with water (2 × 10 mL) to remove NH₄Cl and lastly diethyl ether (2 × 10 mL). A yield of 120 mg (92.9%) of yellow crystals of $[\text{Pt}(\text{[9]aneS}_3)(\text{dpae})](\text{PF}_6)_2$ was obtained. Anal. Found: C, 33.52; H, 3.08; S, 8.37. C₃₂H₃₆As₂F₁₂P₂PtS₃ requires C, 33.37; H, 3.15; S, 8.35. δ_{H} (400 MHz, CD₃NO₂): 7.78–7.62 (m, 20H, *Ph*), 3.12 (s with ¹⁹⁵Pt satellites (³J_{Pt-H} = 14 Hz), 4H, –As–CH₂–CH₂–As–), 2.99–2.85, (m, 6H, [9]aneS₃). 2.72–2.56 (m, 6H, [9]aneS₃). δ_{C} (100 MHz, CD₃NO₂): 134.26 (4C, *Ph*), 133.57 (³J_{Pt-C} = 13 Hz, 8C, *Ph*), 131.67 (8C, *Ph*), 130.40 (²J_{Pt-C} = 43 Hz, 4C, *Ph*), 35.90 (6C, $\nu_{1/2}$ = 3 Hz, [9]aneS₃), 29.88 (²J_{Pt-C} = 68 Hz), –As–CH₂–CH₂–As–). δ_{Pt} (85.9 MHz, CD₃NO₂): –4771 ($\nu_{1/2}$ = 140 Hz). UV-Vis (CH₃CN, nm ($\epsilon/\text{M}^{-1}\text{cm}^{-1}$)): 402 (184), 288 (1.1 × 10⁴), 261 (2.4 × 10⁴). ν_{max} , cm⁻¹: 3068, 3051, 3012, 2972, 2887, 2867, 1478, 1430, 1410, 1302, 1186, 1138, 1059, 1019, 835 (s, PF₆⁻), 732, 689, 665, 551 (s, PF₆⁻). The complex shows no oxidative electrochemistry, but does show an irreversible reduction wave at –1550 mV vs. Fc/Fc+.

[Pd([9]aneS₃)(dpae)](PF₆)₂ (6). The compound was prepared using a procedure identical to compound **5** using the following stoichiometric quantities: $[\text{Pd}(\text{[9]aneS}_3)\text{Cl}_2]$ (50.0 mg, 0.140 mmol), dpae (70.0 mg, 0.144 mmol) and NH₄PF₆ (46 mg, 0.282 mmol). The palladium complex went into solution producing a clear, pale-

orange liquid. The reaction flask was allowed to cool slightly before the addition of the hexafluorophosphate salt. An orange solution was present which was refluxed for an additional 30 min. Cooling overnight resulted in the precipitation of NH₄Cl. These crystals were removed by filtration and the solution concentrated to 2/3 of their original volume. Diethyl ether was slowly diffused (1 wk) into the concentrated orange-red solution resulting in pink needles. The clear, colorless supernatant solution was decanted, and the crystals rinsed twice with 10 mL of diethyl ether. A mass of 81.0 mg of **6** (79.4%) was recovered. Anal. Found: C, 36.21; H, 3.37; S, 9.08. C₃₂H₃₆As₂F₁₂P₂PdS₃ requires C, 36.16; H, 3.41; S, 9.05. δ_{H} (400 MHz, CD₃NO₂): 7.77–7.61 (m, 20H, *Ph*), 3.38 (s, 4H, –As–CH₂–CH₂–As–), 3.06–2.95 (m, 6H, [9]aneS₃). 2.72–2.60 (m, 6H, [9]aneS₃). δ_{C} (100 MHz, CD₃NO₂): 134.36 (4C, *Ph*), 133.53 (8C, *Ph*), 131.85 (8C, *Ph*), 131.33 (4C, *Ph*), 35.75 (6C, $\nu_{1/2}$ = 3 Hz, [9]aneS₃), 30.64 (2C, –As–CH₂–CH₂–As–). UV-Vis (CH₃CN, nm ($\epsilon/\text{M}^{-1}\text{cm}^{-1}$)): 466 (260), 311 (2.4 × 10⁴), 274 (2.0 × 10⁴). ν_{max} , cm⁻¹: 3080, 3053, 2995, 2946, 2925, 2914, 1557, 1471, 1435, 1401, 1294, 1181, 1173, 1079, 999, 835 (s, PF₆⁻), 764, 731, 688, 650, 555 (s, PF₆⁻). The complex shows no oxidative electrochemistry, but does show a quasi-reversible reduction wave at –952 mV ($i_{\text{pc}}/i_{\text{pa}}$ = 0.57) and an irreversible wave at –1406 vs. Fc/Fc+.

X-Ray structural determinations†

Crystals suitable for X-ray diffraction studies were obtained by slow diffusion (several days) of diethyl ether into a concentrated nitromethane solution for compounds **1** and **2**, into a nitromethane–chloroform solution for compounds **3**, and **4**, into acetonitrile for compound **5**, and into acetone for compound **6**. Table 1 contains crystal data, collection parameters, and refinement criteria for the structures of **1**–**6**. For all structures, X-ray intensity data were measured at low temperature with graphite-monochromated radiation (λ = 0.71073 Å) on a Rigaku AFC8S diffractometer equipped with a 1 K Mercury CCD detector. The structure was solved using direct methods and refinement was done using full-matrix least-squares techniques (on F^2).⁴⁶ Data were corrected for absorption, using semi-empirical methods. Structure solution, refinement and the calculation of derived results were performed with the SHELXTL package of computer programs.⁴⁷

Acknowledgements

Acknowledgements are made to the following organizations for their generous support of this research: the donors of the American Chemical Society Petroleum Research Fund; the Research Corporation, the Grote Chemistry Fund at the University of Tennessee at Chattanooga; the National Science Foundation RUI Program. We thank Professor Daron E. Janzen of St. Catherine's College for his comments.

Notes and references

- W. Levason, G. Reid, Acyclic Arsine, Stibine, and Bismuthine Ligands, in *Comprehensive Coordination Chemistry II, Volume 1*, ed. A. B. P. Lever, Elsevier, Amsterdam, 2004, pp. 377–387.
- W. Levason and G. Reid, *Coord. Chem. Rev.*, 2006, **250**, 2565.
- J. C. Cloyd, Jr., C. A. McAuliffe, *Transition Metal Complexes of Phosphorus, Arsenic, and Antimony Ligands*, ed. C. A. McAuliffe, John Wiley and Sons, New York, 1973, p. 205.

- 4 E. C. Alyea, in *Transition Metal Complexes of Phosphorus, Arsenic, and Antimony Ligands*, ed. C. A. McAuliffe, John Wiley and Sons, New York, 1973, p. 311.
- 5 N. R. Champness and W. Levason, *Coord. Chem. Rev.*, 1994, **133**, 115.
- 6 C. A. Tolman, *Chem. Rev.*, 1977, **77**, 313.
- 7 R. H. E. Hudson and A. J. Poe, *Organometallics*, 1995, **14**, 3238.
- 8 H. Nikol, Hans-Beat Bürgi, K. I. Hardcastle and H. B. Gray, *Inorg. Chem.*, 1995, **34**, 6319.
- 9 G. J. Grant, K. N. Patel, M. L. Helm, L. F. Mehne, D. W. Klinger and D. G. VanDerveer, *Polyhedron*, 2004, **23**, 1361.
- 10 T. W. Green, R. Lieberman, N. Mitchell, J. A. Krause Bauer and W. B. Connick, *Inorg. Chem.*, 2005, **44**, 1955.
- 11 D. E. Janzen, K. P. Patel, D. G. VanDerveer and G. J. Grant, *J. Chem. Crystallogr.*, 2006, **36**, 83.
- 12 A. J. Blake, A. J. Holder, T. I. Hyde, Y. V. Roberts, A. J. Lavery and M. Schröder, *J. Organomet. Chem.*, 1987, **323**, 261.
- 13 M. A. Bennett, A. J. Canty, J. K. Felixberger, L. M. Rendina, C. Sunderland and A. C. Willis, *Inorg. Chem.*, 1993, **32**, 1951.
- 14 G. J. Grant, C. G. Brandow, D. F. Galas, J. P. Davis, W. T. Pennington, J. D. Zubkowski and E. J. Valente, *Polyhedron*, 2001, **20**, 3333.
- 15 G.-H. Lee, *Acta Crystallogr.*, 1998, **C54**, 906.
- 16 D. R. Allan, A. J. Blake, D. Huang, T. J. Prior and M. Schröder, *Chem. Commun.*, 2006, 4081.
- 17 D. E. Janzen, L. F. Mehne, D. G. VanDerveer and G. J. Grant, *Inorg. Chem.*, 2005, **44**, 8182.
- 18 D. E. Janzen, D. G. VanDerveer, L. F. Mehne, A. A. da Dilva Fihlo, J.-L. Bredas and G. J. Grant, *Dalton Trans.*, 2008, 1872.
- 19 A. J. Blake, Y. V. Roberts and M. Schröder, *J. Chem. Soc., Dalton Trans.*, 1996, 1885.
- 20 G. J. Grant, I. M. Poullaos, D. F. Galas, D. G. VanDerveer, J. D. Zubkowski and E. J. Valente, *Inorg. Chem.*, 2001, **40**, 564.
- 21 G. J. Grant, S. M. Carter, A. L. Russell, I. M. Poullaos and D. G. VanDerveer, *J. Organomet. Chem.*, 2001, **637–639**, 683.
- 22 G. J. Grant, D. F. Galas and D. G. VanDerveer, *Polyhedron*, 2002, **21**, 879.
- 23 G. J. Grant, D. F. Galas, I. M. Poullaos, S. M. Carter and D. G. VanDerveer, *J. Chem. Soc., Dalton Trans.*, 2002, 2973.
- 24 G. J. Grant, J. P. Pool and D. G. VanDerveer, *Dalton Trans.*, 2003, 3981.
- 25 G. J. Grant, D. A. Biggers and D. G. VanDerveer, *Main Group Chem.*, 2007, **6**, 249.
- 26 A. J. Blake, R. O. Gould, A. J. Holder, T. I. Hyde, A. J. Lavery, M. O. Odulate and M. Schröder, *J. Chem. Soc., Chem. Commun.*, 1987, 118.
- 27 G. J. Grant, N. S. Spangler, L. F. Mehne, W. N. Setzer and D. G. VanDerveer, *Inorg. Chim. Acta*, 1996, **246**, 31.
- 28 H. Jude, J. A. Krause Bauer and W. B. Connick, *J. Am. Chem. Soc.*, 2003, **125**, 3446.
- 29 E. Becker, C. Slugov, E. Rüba, C. Stadfest-Huaser, K. Mereiter, R. Schmid and K. Kirchner, *J. Organomet. Chem.*, 2002, **649**, 55.
- 30 J. E. Huheey, E. A. Keiter, R. L. Keiter, *Inorganic Chemistry, 4th Ed.*, Harper Collins, New York, 1993, p. 292.
- 31 A. W. Addison, T. N. Rao, J. Reedijk, J. van Rijn and G. C. Verschoor, *J. Chem. Soc., Dalton Trans.*, 1984, 1349.
- 32 I. Dance and M. Scudder, *J. Chem. Soc., Chem. Commun.*, 1995, 1039.
- 33 I. Dance and M. Scudder, *J. Chem. Soc., Dalton Trans.*, 2000, 1587.
- 34 G. R. Lewis and I. Dance, *Inorg. Chim. Acta*, 2000, **306**, 160.
- 35 *Cambridge Structural Database v 5.30*, November 2008, Cambridge Crystallographic Data Centre, 12 Union Road, Cambridge CB2 1EZ, UK.
- 36 C. A. McAuliffe, S. E. Niven and R. V. Parish, *Inorg. Chim. Acta*, 1975, **15**, 67.
- 37 F. F. Fanizzi, L. Maresca, G. Natile, M. Lanfranchi, A. Tiripicchio and G. Pacchioni, *J. Chem. Soc., Chem. Commun.*, 1992, 333.
- 38 O. F. Wendt, A. Scodinu and L. I. Elding, *Inorg. Chim. Acta*, 1998, **277**, 237.
- 39 P. Sharma, A. Carbrera, M. Sharma, C. Alvarez, J. L. Arias, R. M. Gomez and S. Hernandez, *Z. Anorg. Allg. Chem.*, 2000, **626**, 2330.
- 40 S. Otto and M. H. Johansson, *Inorg. Chim. Acta*, 2002, **329**, 135.
- 41 P. L. Goggin, R. J. Knight, L. Sinderllari and L. M. Venanzi, *Inorg. Chim. Acta*, 1971, **5**, 62.
- 42 D. F. Shriver, P. W. Atkins, T. L. Overton, J. P. Rourke, M. T. Weller, F. A. Armstrong, *Shriver & Atkins: Inorganic Chemistry*, W. H. Freeman and Company, New York, 4th edn, 2006, p. 461.
- 43 G. J. Grant, *Inorg. Syntheses*, 2009, in review.
- 44 P. S. Pregosin, *Transition Metal Nuclear Magnetic Resonance*, Elsevier, New York, 1991, p. 251, and references cited therein.
- 45 G. J. Grant, D. A. Benefield, D. G. VanDerveer, manuscript in preparation.
- 46 (a) *CrystalClear*, Rigaku/MS, The Woodlands, TX, USA, 1999; (b) R. A. Jacobson, *REQAB, subroutine of CrystalClear*, Rigaku/MS, The Woodlands, TX, USA, 1999.
- 47 G. M. Sheldrick, *SHELXTL 5.1 1998–1999*, Bruker AXS, Madison, WI, USA.